Limits on Quark Compositeness from High Energy Jets in $\bar{p}p$ Collisions at 1.8 TeV

B. Abbott,[48] M. Abolins,[45] V. Abramov,[21] B.S. Acharya,[15] D.L. Adams,[55] M. Adams,[32]
V. Akimov,[19] G.A. Alves,[2] N. Amos,[44] E.W. Anderson,[37] M.M. Baarmand,[50]
V.V. Babintsev,[21] L. Babukhadia,[50] A. Baden,[41] B. Baldin,[31] S. Banerjee,[15] J. Bantly,[54]
E. Barberis,[24] P. Baringer,[38] J.F. Bartlett,[31] U. Bassler,[11] A. Bean,[38] A. Belyaev,[20]
S.B. Beri,[13] G. Bernardi,[11] I. Bertram,[22] V.A. Bezzubov,[21] P.C. Bhat,[31] V. Bhatnagar,[13]
M. Bhattacharjee,[50] G. Blazey,[33] S. Blessing,[29] A. Boehnlein,[31] N.I. Bojko,[21]
F. Borcherding,[31] A. Brandt,[55] R. Breedon,[25] G. Briskin,[54] R. Brock,[45] G. Brooijmans,[31]
A. Bross,[31] D. Buchholz,[34] M. Buehler,[32] V. Buescher,[49] V.S. Burtovoi,[21] J.M. Butler,[42]
F. Canelli,[49] W. Carvalho,[3] D. Casey,[45] Z. Casilum,[50] H. Castilla-Valdez,[17]
D. Chakraborty,[50] K.M. Chan,[49] S.V. Chekulaev,[21] D.K. Cho,[49] S. Choi,[28] S. Chopra,[51]
B.C. Choudhary,[28] J.H. Christenson,[31] M. Chung,[32] D. Claes,[46] A.R. Clark,[24]
J. Cochran,[28] L. Coney,[36] B. Connolly,[29] W.E. Cooper,[31] D. Coppage,[38] D. Cullen-Vidal,[54]
M.A.C. Cummings,[33] D. Cutts,[54] O.I. Dahl,[24] K. Davis,[23] K. De,[55] K. Del Signore,[44]
M. Demarteau,[31] D. Denisov,[31] S.P. Denisov,[21] H.T. Diehl,[31] M. Diesburg,[31]
G. Di Loreto,[45] S. Doulas,[43] P. Draper,[55] Y. Ducros,[12] L.V. Dudko,[20] S.R. Dugad,[15]
A. Dyshkant,[21] D. Edmunds,[45] J. Ellison,[28] V.D. Elvira,[31] R. Engelmann,[50] S. Eno,[41]
G. Eppley,[57] P. Ermolov,[20] O.V. Eroshin,[21] J. Estrada,[49] H. Evans,[47] V.N. Evdokimov,[21]
T. Fahland,[27] S. Feher,[31] D. Fein,[23] T. Ferbel,[49] H.E. Fisk,[31] Y. Fisyak,[51] E. Flattum,[31]
F. Fleuret,[24] M. Fortner,[33] K.C. Frame,[45] S. Fuess,[31] E. Gallas,[31] A.N. Galyaev,[21]
P. Gartung,[28] V. Gavrilov,[19] R.J. Genik II,[22] K. Genser,[31] C.E. Gerber,[31] Y. Gershtein,[54]
B. Gibbard,[51] R. Gilmartin,[29] G. Ginther,[49] B. Gómez,[5] G. Gómez,[41] P.I. Goncharov,[21]
J.L. González Solís,[17] H. Gordon,[51] L.T. Goss,[56] K. Gounder,[28] A. Goussiou,[50] N. Graf,[51]
P.D. Grannis,[50] J.A. Green,[37] H. Greenlee,[31] S. Grinstein,[1] P. Grudberg,[24] S. Grünendahl,[31]
G. Guglielmo,[53] A. Gupta,[15] S.N. Gurzhiev,[21] G. Gutierrez,[31] P. Gutierrez,[53] N.J. Hadley,[41]
H. Haggerty,[31] S. Hagopian,[29] V. Hagopian,[29] K.S. Hahn,[49] R.E. Hall,[26] P. Hanlet,[43]
S. Hansen,[31] J.M. Hauptman,[37] C. Hays,[47] C. Hebert,[38] D. Hedin,[33] A.P. Heinson,[28]
U. Heintz,[42] T. Heuring,[29] R. Hirosky,[32] J.D. Hobbs,[50] B. Hoeneisen,[8] J.S. Hoftun,[54]
A.S. Ito,[31] S.A. Jerger,[45] R. Jesik,[35] T. Joffe-Minor,[34] K. Johns,[23] M. Johnson,[31]
A. Jonckheere,[31] M. Jones,[30] H. Jöstlein,[31] A. Juste,[31] S. Kahn,[51] E. Kajfasz,[10]
D. Karmanov,[20] D. Karmgard,[36] R. Kehoe,[36] S.K. Kim,[16] B. Klima,[31] C. Klopfenstein,[25]
B. Knuteson,[24] W. Ko,[25] J.M. Kohli,[13] A.V. Kostritskiy,[21] J. Kotcher,[51] A.V. Kotwal,[47]
A.V. Kozelov,[21] E.A. Kozlovsky,[21] J. Krane,[37] M.R. Krishnaswamy,[15] S. Krzywdzinski,[31]
M. Kubantsev,[39] S. Kuleshov,[19] Y. Kulik,[50] S. Kunori,[41] G. Landsberg,[54] A. Leflat,[20]
F. Lehner,[31] J. Li,[55] Q.Z. Li,[31] J.G.R. Lima,[3] D. Lincoln,[31] S.L. Linn,[29] J. Linnemann,[45]
R. Lipton,[31] J.G. Lu,[4] A. Lucotte,[50] L. Lueking,[31] C. Lundstedt,[46] A.K.A. Maciel,[33]
R.J. Madaras,[24] V. Manankov,[20] S. Mani,[25] H.S. Mao,[4] T. Marshall,[35] M.I. Martin,[31]
R.D. Martin,[32] K.M. Mauritz,[37] B. May,[34] A.A. Mayorov,[35] R. McCarthy,[50] J. McDonald,[29]
T. McMahon,[52] H.L. Melanson,[31] X.C. Meng,[4] M. Merkin,[20] K.W. Merritt,[31] C. Miao,[54]
H. Miettinen,[57] D. Mihalcea,[53] A. Mincer,[48] C.S. Mishra,[31] N. Mokhov,[31] N.K. Mondal,[15]
H.E. Montgomery,[31] M. Mostafa,[1] H. da Motta,[2] E. Nagy,[10] F. Nang,[23] M. Narain,[42]

V.S. Narasimham,[15] H.A. Neal,[44] J.P. Negret,[5] S. Negroni,[10] D. Norman,[56] L. Oesch,[44]
V. Oguri,[3] B. Olivier,[11] N. Oshima,[31] P. Padley,[57] L.J. Pan,[34] A. Para,[31] N. Parashar,[43]
R. Partridge,[54] N. Parua,[9] M. Paterno,[49] A. Patwa,[50] B. Pawlik,[18] J. Perkins,[55]
M. Peters,[30] R. Piegaia,[1] H. Piekarz,[29] B.G. Pope,[45] E. Popkov,[36] H.B. Prosper,[29]
S. Protopopescu,[51] J. Qian,[44] P.Z. Quintas,[31] R. Raja,[31] S. Rajagopalan,[51] N.W. Reay,[39]
S. Reucroft,[43] M. Rijssenbeek,[50] T. Rockwell,[45] M. Roco,[31] P. Rubinov,[31] R. Ruchti,[36]
J. Rutherfoord,[23] A. Santoro,[2] L. Sawyer,[40] R.D. Schamberger,[50] H. Schellman,[34]
A. Schwartzman,[1] J. Sculli,[48] N. Sen,[57] E. Shabalina,[20] H.C. Shankar,[15] R.K. Shivpuri,[14]
D. Shpakov,[50] M. Shupe,[23] R.A. Sidwell,[39] V. Simak,[7] H. Singh,[28] J.B. Singh,[13]
V. Sirotenko,[33] P. Slattery,[49] E. Smith,[53] R.P. Smith,[31] R. Snihur,[34] G.R. Snow,[46]
J. Snow,[52] S. Snyder,[51] J. Solomon,[32] X.F. Song,[4] V. Sorín,[1] M. Sosebee,[55] N. Sotnikova,[20]
K. Soustruznik,[6] M. Souza,[2] N.R. Stanton,[39] G. Steinbrück,[47] R.W. Stephens,[55]
M.L. Stevenson,[24] F. Stichelbaut,[51] D. Stoker,[27] V. Stolin,[19] D.A. Stoyanova,[21]
M. Strauss,[53] K. Streets,[48] M. Strovink,[24] L. Stutte,[31] A. Sznajder,[3] W. Taylor,[50]
S. Tentindo-Repond,[29] T.L.T. Thomas,[34] J. Thompson,[41] D. Toback,[41] T.G. Trippe,[24]
A.S. Turcot,[44] P.M. Tuts,[47] P. van Gemmeren,[31] V. Vaniev,[21] R. Van Kooten,[35]
N. Varelas,[32] A.A. Volkov,[21] A.P. Vorobiev,[21] H.D. Wahl,[29] H. Wang,[34] J. Warchol,[36]
G. Watts,[58] M. Wayne,[36] H. Weerts,[45] A. White,[55] J.T. White,[56] D. Whiteson,[24]
J.A. Wightman,[37] S. Willis,[33] S.J. Wimpenny,[28] J.V.D. Wirjawan,[56] J. Womersley,[31]
D.R. Wood,[43] R. Yamada,[31] P. Yamin,[51] T. Yasuda,[31] K. Yip,[31] S. Youssef,[29] J. Yu,[31]
Z. Yu,[34] M. Zanabria,[5] H. Zheng,[36] Z. Zhou,[37] Z.H. Zhu,[49] M. Zielinski,[49] D. Zieminska,[35]
A. Zieminski,[35] V. Zutshi,[49] E.G. Zverev,[20] and A. Zylberstejn[12]

(DØ Collaboration)

[1] *Universidad de Buenos Aires, Buenos Aires, Argentina*
[2] *LAFEX, Centro Brasileiro de Pesquisas Físicas, Rio de Janeiro, Brazil*
[3] *Universidade do Estado do Rio de Janeiro, Rio de Janeiro, Brazil*
[4] *Institute of High Energy Physics, Beijing, People's Republic of China*
[5] *Universidad de los Andes, Bogotá, Colombia*
[6] *Charles University, Prague, Czech Republic*
[7] *Institute of Physics, Academy of Sciences, Prague, Czech Republic*
[8] *Universidad San Francisco de Quito, Quito, Ecuador*
[9] *Institut des Sciences Nucléaires, IN2P3-CNRS, Universite de Grenoble 1, Grenoble, France*
[10] *CPPM, IN2P3-CNRS, Université de la Méditerranée, Marseille, France*
[11] *LPNHE, Universités Paris VI and VII, IN2P3-CNRS, Paris, France*
[12] *DAPNIA/Service de Physique des Particules, CEA, Saclay, France*
[13] *Panjab University, Chandigarh, India*
[14] *Delhi University, Delhi, India*
[15] *Tata Institute of Fundamental Research, Mumbai, India*
[16] *Seoul National University, Seoul, Korea*
[17] *CINVESTAV, Mexico City, Mexico*
[18] *Institute of Nuclear Physics, Kraków, Poland*
[19] *Institute for Theoretical and Experimental Physics, Moscow, Russia*
[20] *Moscow State University, Moscow, Russia*

[21]Institute for High Energy Physics, Protvino, Russia
[22]Lancaster University, Lancaster, United Kingdom
[23]University of Arizona, Tucson, Arizona 85721
[24]Lawrence Berkeley National Laboratory and University of California, Berkeley, California 94720
[25]University of California, Davis, California 95616
[26]California State University, Fresno, California 93740
[27]University of California, Irvine, California 92697
[28]University of California, Riverside, California 92521
[29]Florida State University, Tallahassee, Florida 32306
[30]University of Hawaii, Honolulu, Hawaii 96822
[31]Fermi National Accelerator Laboratory, Batavia, Illinois 60510
[32]University of Illinois at Chicago, Chicago, Illinois 60607
[33]Northern Illinois University, DeKalb, Illinois 60115
[34]Northwestern University, Evanston, Illinois 60208
[35]Indiana University, Bloomington, Indiana 47405
[36]University of Notre Dame, Notre Dame, Indiana 46556
[37]Iowa State University, Ames, Iowa 50011
[38]University of Kansas, Lawrence, Kansas 66045
[39]Kansas State University, Manhattan, Kansas 66506
[40]Louisiana Tech University, Ruston, Louisiana 71272
[41]University of Maryland, College Park, Maryland 20742
[42]Boston University, Boston, Massachusetts 02215
[43]Northeastern University, Boston, Massachusetts 02115
[44]University of Michigan, Ann Arbor, Michigan 48109
[45]Michigan State University, East Lansing, Michigan 48824
[46]University of Nebraska, Lincoln, Nebraska 68588
[47]Columbia University, New York, New York 10027
[48]New York University, New York, New York 10003
[49]University of Rochester, Rochester, New York 14627
[50]State University of New York, Stony Brook, New York 11794
[51]Brookhaven National Laboratory, Upton, New York 11973
[52]Langston University, Langston, Oklahoma 73050
[53]University of Oklahoma, Norman, Oklahoma 73019
[54]Brown University, Providence, Rhode Island 02912
[55]University of Texas, Arlington, Texas 76019
[56]Texas A&M University, College Station, Texas 77843
[57]Rice University, Houston, Texas 77005
[58]University of Washington, Seattle, Washington 98195

Abstract

Events in $\overline{p}p$ collisions at $\sqrt{s} = 1.8$ TeV with total transverse energy exceeding 500 GeV are used to set limits on quark substructure. The data are consistent with next-to-leading order QCD calculations. We set a lower limit of 2.0 TeV at 95% confidence on the energy scale Λ_{LL} for compositeness in quarks, assuming a model with a left-left isoscalar contact interaction term. The limits on Λ_{LL} are found to be insensitive to the sign of the interference term in the Lagrangian.

Typeset using REVTEX

The first limit on the size of the atomic nucleus was obtained by Geiger and Marsden in the Rutherford [1] scattering of α particles from nuclei. In an analogous way, we can set a limit on the size of quarks by observing the scattering of the highest energy quarks and antiquarks at the Fermilab Tevatron Collider at $\overline{p}p$ center-of-mass energies of 1.8 TeV. The scattered quarks from within the proton emerge in the laboratory as collimated showers of hadrons, called jets. The scalar sum of the transverse energies of the jets in any event provides a measure of the hardness (the impact parameter) of collisions. The summed transverse energy of the event is simply expressed

$$H_T \equiv \sum_{i=1}^{N} E_T^i \, ,$$

where N is the number of jets in the event above some threshold, and E_T^i is the transverse energy of jet i, essentially the momentum component of the jet in the plane transverse to the beams [2].

H_T is a robust quantity in the multiple interaction environment of the Tevatron, where often a hard scattering is accompanied by one or more soft interactions that do not produce high E_T jets. Such overlapping events contribute only a small and easily corrected bias to H_T. For individual jets, the precise measurement of the hard-scattering vertex is crucial for determining E_T^i, but changes in E_T^i induced by changing the position of the vertex are partially compensated in H_T. Efficiencies and resolutions are measured as functions of E_T^i; these are correlated weakly with H_T because of an effective averaging over final-state topologies. By treating the event as a whole, this analysis complements the more traditional probes of QCD, such as measurements of the inclusive jet cross section [3,4], the dijet mass spectrum [5], and the dijet angular distribution [6,7]. A measurement of $d\sigma/dH_T$ has been published by the CDF collaboration [8].

This analysis focuses on a test of quark compositeness within the formalism of Eichten *et al.* [9] for events with $H_T > 500$ GeV. In the Lagrangian of Ref. [9], we test for compositeness of left-handed quarks in the left-left isoscalar term,

$$L_{qq} = \mathcal{A}\,(g^2/2\Lambda_{LL}^2)\,\overline{q_L}\gamma^\mu q_L \overline{q_L}\gamma_\mu q_L \, ,$$

where $\mathcal{A} = \pm 1$ is the sign of the interference term, Λ_{LL} is the compositeness scale, and the dependence on α_s is contained in the compositeness coupling constant g^2. The model is completely determined by specifying the two parameters $\mathcal{A}$ and Λ_{LL}. In this model, all three families of quarks are assumed to be composite, and both signs of the interference term (resulting in constructive (-1) and destructive ($+1$) interference) are investigated. In this search for quark compositeness at jet energies well above the mass of the top quark, with $H_T > 500$ GeV $> 2\mathrm{m_t} \approx 350$ GeV, the only backgrounds considered are from instrumental sources. For comparison to these results, Table I shows the previous quark compositeness limits.

The DØ detector is described in detail in Ref. [10]. The principal components of the detector used in this analysis are the calorimeter for measuring jets, and the central tracking system for determining the hard-scattering vertex. The pseudorapidity, $\eta = -\ln(\tan(\theta/2))$, of the calorimeter extends to $|\eta| \leq 4.2$, corresponding to a polar angle relative to the incident proton of $\theta \approx 2^\circ$. The depth of the DØ calorimeter varies from 6 to 10 nuclear interaction lengths, thereby providing good containment for jets. Jet energy resolution is approximately $80\%/\sqrt{E}$, and the resolution on the z-position of the hard-scattering vertex is ±8 mm.

Our analysis is based on 91.9 ± 5.6 pb^{-1} [11] of data taken during the 1994-1995 run of the Tevatron. The hardware trigger required a minimum transverse energy exceeding 45 GeV in a region $\Delta\eta \times \Delta\phi = 0.8 \times 1.6$ of the calorimeter, where ϕ is the azimuthal angle. In addition, beam halo effects from the Main Ring, the preaccelerator to the Tevatron, were minimized through timing restrictions. The software filter required at least one jet with $E_T > 115$ GeV. The combined selection efficiency was found to exceed 99% for events with $H_T > 500$ GeV.

A significant fraction of the data were taken at high instantaneous luminosity, which resulted in more than one $\overline{p}p$ interaction in a beam crossing leading to an ambiguity in selecting the primary event vertex. After event reconstruction, the two vertices with the largest track multiplicity were retained. When there was a second reconstructed vertex in the event, the imbalance in transverse momentum or missing E_T ($\not\!\!E_T$) was calculated using transverse vector energies:

$$\not\!\!E_T \equiv |\sum_{i=1}^{N} \vec{E_T^i}| .$$

This was evaluated for both event vertex candidates, with the primary vertex chosen to minimize $\not\!\!E_T$. The z-position of the vertex was required to satisfy $|z_{vtx}| \leq 50$ cm. The efficiency for this cut was measured to be approximately 90%, independent of H_T.

Offline jet reconstruction used a fixed-cone algorithm with radius

$$\mathcal{R} = \sqrt{(\Delta\eta)^2 + (\Delta\phi)^2} = 0.7\,,$$

and was fully efficient for $E_T > 20$ GeV, the threshold applied to each jet for inclusion in H_T. The jet energy scale corrections applied to the data are described in Ref. [12]. Additional offline cuts were applied to the events to minimize instrumental background and ambiguities in defining E_T^i and $\not\!\!E_T$.

All jets with $E_T > 20$ GeV and with $|\eta^j| < 3.0$ were required to pass jet selection criteria, which included: (i) the electromagnetic fraction of the jet energy, measured in the first layers of the uranium-liquid-argon calorimeter, was required to be between 0.05 and 0.95, except in the region between the central and end cryostats, where only the upper limit was imposed; (ii) the fraction of energy in the outermost hadronic section was required to be < 0.40; and, (iii) the ratio $E_T^{cell\ 1}/E_T^{cell\ 2}$ was required to be < 10, where the calorimeter cells comprising the jet were ordered in decreasing E_T. An event was rejected if any of its jets with $E_T > 20$ GeV failed the quality or η requirements. The efficiency for a jet to pass these criteria was parameterized as a function of E_T, and the efficiency for an event to pass the criteria was essentially independent of H_T above 500 GeV.

The H_T distribution for $H_T > 500$ GeV is shown in Fig.1. The events passed all the above selection criteria and were corrected for efficiencies and jet energy scale, but not for resolution. The cross section falls by three orders-of-magnitude over the range in H_T from $500 - 1000$ GeV. Fig. 2 displays the fractional deviation between the data and the Monte Carlo for the CTEQ4M PDF with a renormalization scale of $E_T^{\max}/2$.

The H_T spectrum expected from the standard model was provided by the JETRAD [13] Monte Carlo event generator, which is based on a next-to-leading order (NLO) QCD calculation. We tried several choices for the renormalization scale μ parameterized as $\mu = f_E \cdot E_T^{\max}$ and $\mu = f_H \cdot H_T$, where f_E and f_H are constants we varied from 0.25 to 1.50. We used two parton distribution functions (PDFs): CTEQ4M [14] and MRST [15].

For Λ_{LL} scales between 1.4 and 7.0 TeV, PYTHIA [16] was used to simulate the effects of quark compositeness to leading order (LO). The results for composite quarks relative to expectations from the standard model are also shown in Fig. 2 for $\Lambda_{LL} = 1.7, 2.0$ and 2.5 TeV. The ratios are independent of the PYTHIA renormalization scale for the range considered here. Using the above ratio from PYTHIA, we scaled the JETRAD calculation for each PDF to obtain our estimate of the expected cross section for any given Λ_{LL}.

As seen in Fig. 2, quark compositeness would show up as a relative rise in the cross section as a function of H_T. Changes in renormalization scale affect the absolute cross section, but not the shape of H_T distribution. Cross sections calculated using CTEQ4M or MRST PDFs differ in normalization but only slightly in shape. Our analysis will therefore be based on comparison of the shapes of the measured and predicted H_T distributions.

The event efficiency depends weakly on H_T, and the corrections are applied directly to the Monte Carlo generated events. The jet energies in the Monte Carlo are smeared according to measured resolution functions. The effect of this smearing is also found to be independent of H_T, resulting in just an overall rescaling of the H_T distribution. Finally, the jet energy scale (and its uncertainty) is used to correct the Monte Carlo and to determine bin-to-bin correlations in H_T. The expected distribution, with a variable normalization, is then compared directly to data.

The error bars in Fig. 2 are statistical, and the envelope indicates the systematic uncertainty (one standard deviation) from the jet energy scale. The systematic uncertainties range from 17% at the lowest bin shown, to 34% at the highest H_T bin. Because these uncertainties are highly correlated ($> 92\%$) in H_T, the line-shape of the H_T distribution is quite constrained within the 95% confidence level (CL) limit. The distribution of (Data−JETRAD)/JETRAD in Fig. 2 exhibits no deviation from QCD. From this measurement, we conclude that there is no evidence for quark compositeness below an energy scale of 2.0 TeV.

A modified Bayesian [17,18] procedure sets the 95% CL lower limits on quark compositeness. The procedure considers the efficiencies, the smearing of jet energy in the Monte Carlo, the integrated luminosity, the uncertainty and correlations on the jet energy scale, and the normalization on the expected cross section. Because the efficiencies, resolutions, and integrated luminosity are independent of H_T, these parameters were included in the normalization, which was defined to have a flat prior probability. A Gaussian prior was assumed for the jet energy scale, and a flat prior for $\xi \equiv 1/\Lambda_{LL}^2$. The standard model corresponds to $\Lambda_{LL} \to \infty$ ($\xi \to 0$). The renormalization scale was varied and the results are summarized in Table II. The 95% confidence level limits are obtained from the ξ distributions by integrating the posterior probability and requiring that 95% of the integral be below the limit. Separate limits for both signs of the interference term and for the two PDFs, CTEQ4M and MRST, are listed in Table II. In general, the limits show small increases for the negative sign of the interference term, and the MRST PDF. The limits also slightly increase with increasing renormalization scale.

We checked the stability of the limits given in Table II. The cut $|\eta^j| \leq 3$ was tightened to $|\eta^j| \leq 2$, thereby excluding events with forward jets in the H_T distribution, with essentially no impact on the limits. Possible bias introduced by our selection of the hard-scattering vertex was studied again, with no observed impact on the limits. The E_T threshold of the jets was increased from 20 GeV to 50 GeV, and the analysis repeated. The resulting limits were consistent with those based on the 20 GeV threshold. Changing the assumed jet energy resolution by ±1 standard deviation had little effect on the shape of the H_T distribution, and thus, little effect on the limit. Varying α_s was investigated through use of the CTEQ4A1-A5 PDFs for a single choice of μ and $\mathcal{A}$, as shown in Table III. There is very little change of the limit for $0.110 \leq \alpha_s \leq 0.122$, corresponding to a Q^2 range from $(50\ \text{GeV})^2$ to $(230\ \text{GeV})^2$. The impact of the gluon content of the proton was studied using the PDF MRST($g\uparrow$) (one standard deviation high) and MRST($g\downarrow$) (one standard deviation low) [15]. The limits shown in Table III depend only weakly on this choice. Finally, the distribution from JETRAD (number of events in each H_T-bin) was fluctuated according to Poisson statistics, and the limit recalculated. The resulting limits were only 0.1 TeV higher than the limits based on the data, providing a measure of the sensitivity of this analysis to the finite statistics and uncertainties in energy-scale.

In summary, the measured H_T distribution above 500 GeV is well modeled by the JETRAD (NLO QCD) event generator. We find no evidence for compositeness in quarks, and set lower limits on the compositeness scale as a function of renormalization scale, sign of the interference term in the compositeness Lagrangian, and choice of PDF. These limits are not affected by small variations in our analysis procedures. The average radius of the scattered quark (principally from the first family) is therefore less than $\Delta x \approx \hbar c/\Lambda_{LL} \approx 1 \times 10^{-4}$ fm.

We thank the staffs at Fermilab and at collaborating institutions for contributions to this work, and acknowledge support from the Department of Energy and National Science Foundation (USA), Commissariat à L'Energie Atomique and CNRS/Institut National de Physique Nucléaire et de Physique des Particules (France), Ministry for Science and Technology and Ministry for Atomic Energy (Russia), CAPES and CNPq (Brazil), Departments of Atomic Energy and Science and Education (India), Colciencias (Colombia), CONACyT (Mexico), Ministry of Education and KOSEF (Korea), CONICET and UBACyT (Argentina), A.P. Sloan Foundation, and the Humboldt Foundation.

REFERENCES

[1] E. Rutherford, J. Chadwick, C. D. Ellis (1930). *Radiations from radioactive substances.* Cambridge University Press.

[2] D. Baden, Int.J.Mod.Phys. **A13**, 1817 (1998).

[3] DØ Collaboration, B. Abbott, *et al.*, Phys. Rev. Lett. **82**, 2451 (1999), hep-ex/9807018.

[4] CDF Collaboration, F. Abe *et al.,* Phys. Rev. Lett. **77**, 438 (1996), hep-ex/9601008.

[5] DØ Collaboration, B. Abbott *et al.,* Phys. Rev. Lett. **82**, 2457 (1999), hep-ex/9807014.

[6] DØ Collaboration, B. Abbott *et al.,* Phys. Rev. Lett. **80**, 666 (1998), hep-ex/9707016.

[7] CDF Collaboration, F. Abe *et al.*, Phys. Rev. Lett. **77**, 5336 (1996). Erratum - *ibid.* **78**, 4307 (1997), hep-ex/9609011.

[8] CDF Collaboration, F. Abe *et al.*, Phys. Rev. Lett. **80**, 3461 (1998), Fermilab-Pub-97-290-E.

[9] E. Eichten, K. Lane and M.E. Peskin, Phys. Rev. Letts. **50**, 811 (1983); E. Eichten, I. Hinchliffe, K. Lane, and C. Quigg, Rev. Mod. Phys. **56**, 579 (1984); ibid., **58**, 1065 (1986); K. Lane, hep-ph/9605257.

[10] DØ Collaboration, S. Abachi *et al.*, Nucl. Instr. & Meth. **A338**, 185 (1994), Fermilab-Pub-93-179-E.

[11] J. Bantly et al., Fermilab-TM-1995 (unpublished). In order to facilitate comparison with previously published results, this analysis does not use the luminosity normalization given in the Dzero Collaboration, B. Abbott et al., Phys. Rev. **D61**, 072001 (2000), sec. VII, hep-ex/9906025. The updated normalization would have the effect of increasing the luminosity by 3.2%.

[12] DØ Collaboration, B. Abbott *et al.,* Nucl. Instr. & Meth. **A424**, 352 (1999), hep-ex/9805009.

[13] W. Giele, E. Glover, and D. Kosower, Nucl. Phys. **B403**, 633 (1993), hep-ph/9302225.

[14] H.L. Lai *et al.,* Phys. Rev. D **55**, 1280 (1997), hep-ph/9606399.

[15] A.D. Martin *et al.,* Eur. Phys. J. C **4** 463 (1998), hep-ph/9803445.

[16] T. Sjöstrand, Comp. Phys. Comm. **82**, 74 (1994). PYTHIA 5.7 only contains the left-left isoscalar model of quark compositeness.

[17] F.T. Solmitz, Ann. Rev. Nucl. Sci. **14**, 375 (1964).

[18] I. Bertram, *et al.,* Fermilab-TM-2104 (unpublished).

TABLE I. Previous 95% CL limits, given in TeV, on the left-left isoscalar quark compositeness model.

Method	Λ^+_{LL}	Λ^-_{LL}
Dijet Mass (DØ) [5]	2.4	2.7
Dijet Angular Distribution (DØ) [6]	2.1	2.2
Dijet Angular Distribution (CDF) [7]	1.8	1.6

TABLE II. The 95% CL lower limits on quark compositeness in TeV, for both CTEQ4M and MRST PDFs, and for renormalization scales $\mu = f_E \cdot E_T^{\max}$ and $\mu = f_H \cdot H_T$ (where $E_T^{\max}$ is for the leading jet). For each PDF, the first limit is for $\mathcal{A} = +1$ and the second is for $\mathcal{A} = -1$.

f_E	CTEQ4M		MRST		f_H	CTEQ4M		MRST	
	Λ^+_{LL}	Λ^-_{LL}	Λ^+_{LL}	Λ^-_{LL}		Λ^+_{LL}	Λ^-_{LL}	Λ^+_{LL}	Λ^-_{LL}
0.25	1.9	1.9	1.9	2.0	0.25	1.9	2.0	2.0	2.1
0.50	1.9	2.0	2.0	2.1	0.50	2.0	2.0	2.1	2.2
0.75	2.0	2.0	2.0	2.1	0.75	2.0	2.1	2.1	2.2
1.00	2.0	2.0	2.1	2.2	1.00	2.0	2.1	2.1	2.2
1.25	2.0	2.0	2.1	2.2					
1.50	2.0	2.1	2.1	2.2					

TABLE III. The 95% CL lower limits on quark compositeness scale in Λ_{LL}(TeV) for different α_s (CTEQ4A1-5) and different gluon content (MRST($g\uparrow$) and MRST($g\downarrow$)). The renormalization scale is $E_T^{\max}/2$, $\mathcal{A}=+1$. The limits for CTEQ4M and MRST are included for comparison.

PDF	Λ^+_{LL}	PDF	Λ^+_{LL}	PDF	Λ^+_{LL}
CTEQ4A1	2.0	CTEQ4A2	2.0	CTEQ4M	1.9
CTEQ4A4	1.9	CTEQ4A5	1.9		
MRST($g\uparrow$)	2.0	MRST($g\downarrow$)	2.1	MRST	2.0

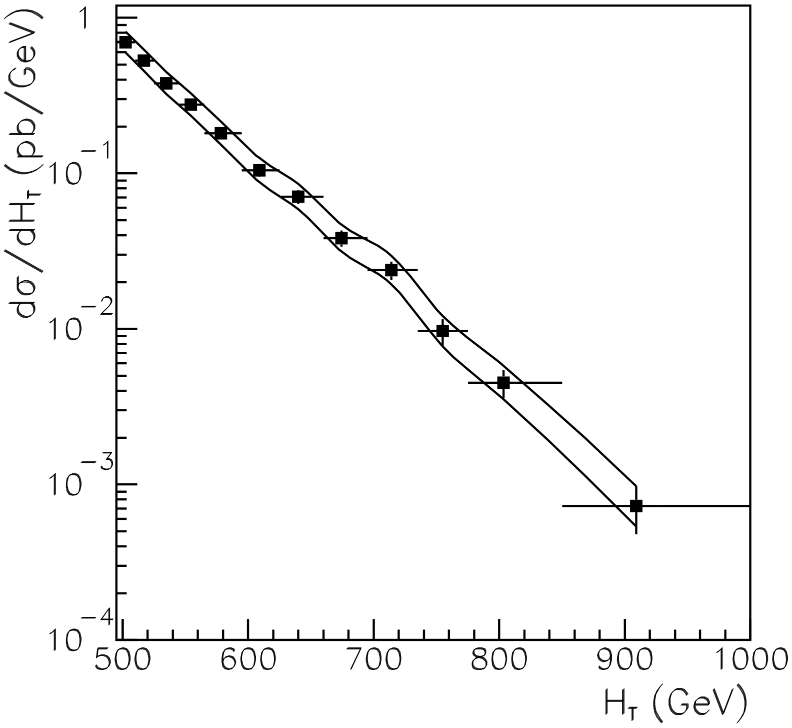

FIG. 1. The H_T distribution for H_T above 500 GeV. Error bars are statistical, and the error envelope shows the systematic error on the jet-energy scale. This cross section is corrected for efficiencies and jet energy scale, but not for resolution.

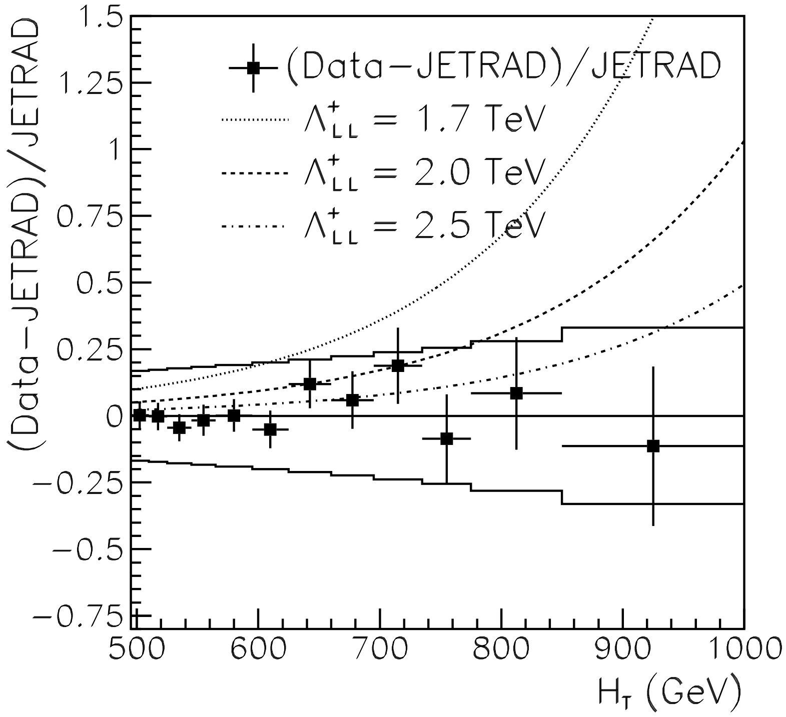

FIG. 2. Comparison of the measured H_T distribution with JETRAD (CTEQ4M and a renormalization scale of $\mu = E_T^{\max}/2$). The errors on the points are statistical, and the error band represents the highly correlated systematic uncertainty due to the jet energy scale. The superimposed curves correspond to expectations for three compositeness scales.